Inorganic Chemistry

pubs.acs.org/IC

Article

Lanthanide 5,7-Disulfonate-1,4-naphthalenedicarboxylate Frameworks Constructed from Trinuclear and Tetranuclear Lanthanide Carboxylate Clusters: Proton Conduction and Selective Fluorescent Sensing of Fe^{3+}

Meng-Ye Xu, Yu-Ling Wang,* Qingyou Liu, Zhao-Ting Lin, and Qing-Yan Liu*

Cite This: https://dx.doi.org/10.1021/acs.inorgchem.0c00680

Read Online

ACCESS | Metrics & More | Article Recommendations | Supporting Information

ABSTRACT: The novel sulfonate-carboxylate ligand of 5,7-disulfonate-1,4-naphthalenedicarboxylic acid (H_4-DSNPDC) was synthesized, and its series of lanthanide compounds $\{[Ln_3(\mu_2\text{-}OH)(DSNPDC)_2(H_2O)_x]\cdot yH_2O\}_n$ (**JXNU-7**; Ln = La^{3+}, x = 10. y = 4; Ln = Nd^{3+}, Sm^{3+} Eu^{3+}, x = 9, y = 2) and $\{[Ln_4(\mu_3\text{-}OH)_4(DSNPDC)_2(H_2O)_{11}]\cdot 28H_2O\}_n$ (**JXNU-8**; Ln = Eu^{3+}, Gd^{3+}) are presented. **JXNU-7** is a three-dimensional structure based on linear trinuclear Ln_3 building units, while **JXNU-8** has a two-dimensional layer constructed from tetranuclear $Ln_4(\mu_3\text{-}OH)_4$ building units. The representative Eu compounds of **JXNU-7** and **-8** show good proton conductive properties under high humidity. The hydrophilic sulfonate groups pointing to the pores and the water molecules included in the pores mainly contribute to the high proton conductivity for the materials. The presence of one-dimensional infinite hydrogen-bonded networks in channels of **JXNU-7**(Eu) facilitates a fast and efficient proton transfer, resulting in higher proton conductivity in comparison to that of **JXNU-8**(Eu). Additionally, **JXNU-7**(Eu) with a characteristic red emission exhibits a promising potential for selective sensing of Fe^{3+} ions in aqueous solution. Our work demonstrates the integration of functional organic components (sulfonate groups) and inorganic components (lanthanide centers) in MOFs for the successful preparation of multifunctional MOF materials.

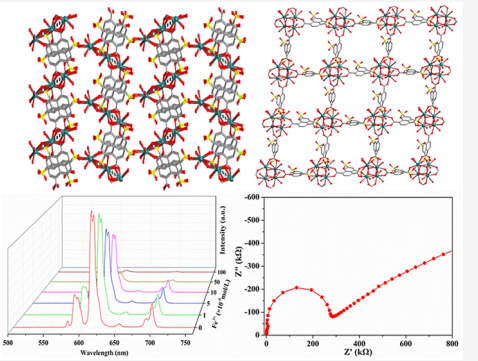

INTRODUCTION

Metal−organic frameworks (MOFs) constructed from organic ligands and metal ions through coordination bonds are an important class of interesting crystalline materials. In the past few decades, MOFs have shown a broad spectrum of applications in gas adsorption/separation,[1] photoluminescence,[2] sensing,[3] proton conduction,[4] and molecular magnets.[5] Due to the crystalline nature of MOFs, the functional building units with magnetism, luminescence, or electricity can be easily introduced into the MOFs. As an important component of MOFs, the organic linker plays a decisive role in the functional ability of MOFs. For example, a three-dimensional (3D) compound based on a 2-sulfonylterephthalate ligand exhibits sorption performance for acidic molecules, which is the result of the abundant basic $-SO_3^-$ groups on the pore walls of the structure.[6] On the introduction of different functional groups into the terephthalate ligand in the UiO-66 system, the sulfonate- or carboxylate-functionalized UiO-66 compounds were found to be have higher proton conductivity in comparison to other UiO-66 series. Such a result is primarily the result of the high hydrophilicity and acidity of the sulfonate and carboxylate groups.[7] On the other hand, the inorganic components of metal centers can endow MOFs with desirable magnetic and luminescent properties. Well-known examples are the lanthanide-based MOFs displaying characteristic lanthanide emissions derived from the intrinsic 4f electron configurations of the lanthanide centers.[8] The large numbers of lanthanide MOFs serving as luminescence sensors for the recognition of various guests are well documented.[9] The lanthanide ions have a strong affinity for oxygen; therefore, the oxygen-containing carboxylate ligands have been broadly investigated as organic linkers for the construction of lanthanide-based MOFs.[10] In contrast to carboxylate ligands, the sulfonate ligands have been much less explored for building MOFs. The ligands containing a sulfonate group with three oxygen atoms provide potential candidates for the construction of lanthanide-based MOFs. However, the weak binding nature of the sulfonate group leads to low robustness of the lanthanide sulfonate frameworks.[11] The combination of

Received: March 4, 2020

sulfonate and carboxylate functional groups within a ligand provides an interesting kind of organic ligand.[12] In this paper, a new ligand of 5,7-disulfonate-1,4-naphthalenedicarboxylic acid (H_4-DSNPDC) was prepared. Six lanthanide compounds, namely, $\{[Ln_3(\mu_2\text{-}OH)(DSNPDC)_2(H_2O)_x]\cdot yH_2O\}_n$ (**JXNU-7**; Ln = La^{3+}, $x = 10$, $y = 4$; Ln = Nd^{3+}, Sm^{3+}, Eu^{3+}, $x = 9$, $y = 2$) and $\{[Ln_4(\mu_3\text{-}OH)_4(DSNPDC)_2(H_2O)_{11}]\cdot 28H_2O\}_n$ (**JXNU-8**, Ln = Eu^{3+} and Gd^{3+}), based on the $DSNPDC^{4-}$ ligand are presented. The hydrophilic nature of sulfonate groups with fast proton transmission character endows the Eu analogues with high proton conductivity under high humidity. The largest proton conductivities for **JXNU-7**(Eu) and **JXNU-8**(Eu) are 1.04×10^{-4} and 2.28×10^{-5} S cm^{-1}, respectively. The Cu(II) and Cd(II) 5-sulfoisophthalate compounds with additional N,N′-donor linkers show proton conductivities in the range of 10^{-5}–10^{-8} S cm^{-1}.[13] The tetranuclear copper(II) cluster or terbium(III) cluster based MOFs with sulfonate-carboxylate ligands have proton conductivities of 10^{-4} S cm^{-1}.[14] A Cr 4,8-disulfonaphthalene-2,6-dicarboxylate compound featuring 1D channels lined with sulfonate groups shows a high proton conductivity of 10^{-2} S cm^{-1}.[12a] Furthermore, **JXNU-7**(Eu) with characteristic Eu^{3+} emission is found to be a potential sensor for selective Fe^{3+} detection among trivalent metal ions. Thus, the functionalities endowed by the organic and inorganic building units are successfully assembled in the resulting MOFs.

EXPERIMENTAL SECTION

Chemicals. All chemicals were commercially obtained except for 5,7-disulfonate-1,4-naphthalenedicarboxylic acid (H_4-DSNPDC), which was synthesized as follows (Scheme 1).

Scheme 1. Synthesis of 5,7-Disulfonate-1,4-naphthalenedicarboxylic Acid Ligand

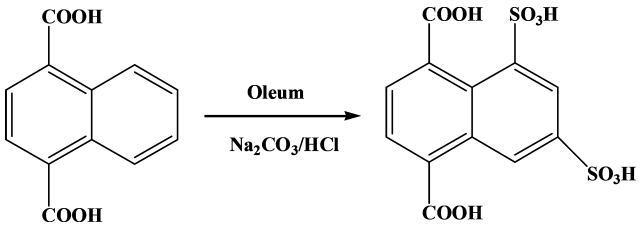

Synthesis of 5,7-Disulfonate-1,4-naphthalenedicarboxylic Acid. A 1.0 g portion of 1,4-naphthalenedicarboxylic acid was placed in a 50 mL three-necked round-bottom flask with 6 mL of 30% oleum at room temperature. The mixture was stirred at 130 °C for 10 h. After it was cooled to room temperature, the mixture was poured into ice water. The resulting mixture was filtered to give a filtrate and precipitate. The precipitate was washed with 1 M Na_2CO_3 aqueous solution, and the obtained mixture was filtered. The two parts of the filtrates were combined and then transferred into a round-bottom flask. The combined filtrate was acidified by 1 M HCl to give the pale yellow product. Yield: ∼79% based on 1,4-naphthalenedicarboxylic acid. ^{1}H NMR (methanol-d_4, ppm): 9.45 (s, 1H), 8.87 (s, 1H), 8.11 (s, 1H), 7.99 (s, 1H). IR (cm^{-1}, KBr pellet): 3497 (s), 1723 (s), 1638 (m), 1573 (w), 1497 (m), 1445 (m), 1398 (m), 1371 (w), 1262 (s), 1240 (s), 1184 (s), 1135 (m), 1072 (m), 1047 (s), 1024 (m), 973 (w), 877 (w), 821 (w), 762 (m), 705 (w), 677 (w), 637 (s), 622 (s), 588 (w), 544 (w).

Synthesis of $\{[La_3(\mu_2\text{-}OH)(DSNPDC)_2(H_2O)_{10}]\cdot 4H_2O\}_n$ and $\{[Ln_3(\mu_2\text{-}OH)(DSNPDC)_2(H_2O)_9]\cdot 2H_2O\}_n$ (JXNU-7; Ln = Nd^{3+}, Sm^{3+}, Eu^{3+}). The synthetic procedures of the four compounds are similar. Typically, $Ln(NO_3)_3\cdot 6H_2O$ (0.025 mmol), 5,7-disulfonate-1,4-naphthalenedicarboxylic acid (9.4 mg, 0.025 mmol), and H_2O (3 mL) were transferred into a 20 mL Parr Teflon-lined stainless steel vessel, which was capped tightly and warmed to 120 °C for 3 days. Crystalline products were observed after cooling to room temperature. The crystals were filtered and dried in air. Yield based on the $Ln(NO_3)_3\cdot 6H_2O$ species: 25% for **JXNU-7**(La); 47% for **JXNU-7**(Nd); 8% for **JXNU-7**(Sm); 56% for **JXNU-7**(Eu). Anal. Calcd/found for $C_{24}H_{37}O_{35}S_4La_3$ (1430.50): H, 2.60/2.56; C, 20.15/20.21; S, 8.96/9.03; La, 29.13/29.22. Calcd/found for $C_{24}H_{31}O_{32}S_4Nd_3$ (1392.45): H, 2.24/2.12; C, 20.70/20.76; S, 9.21/9.26; Nd, 31.07/29.92. Calcd/found for $C_{24}H_{31}O_{32}S_4Eu_3$ (1415.61): H, 2.20/2.16; C, 20.36/20.43; S, 9.06/9.15; Eu, 32.20/32.12. IR (cm^{-1}, KBr pellet): **JXNU-7**(La), 3438 (s), 1595 (s), 1536 (s), 1499 (s), 1448 (m), 1399 (s), 1375 (w), 1339 (m), 1223 (w), 1182 (w), 1074 (m), 1040 (s), 1027 (w), 871 (m), 842 (m), 812 (w), 784 (m), 764 (w), 754 (w), 686 (m), 632 (m), 582 (w), 555 (w), 541 (w), 520 (w), 497 (w), 452 (w), 425 (w); **JXNU-7**(Nd), 3739 (w), 3452 (s), 1608 (s), 1596 (w), 1540 (s), 1448 (m), 1402 (s), 1376 (w), 1340 (m), 1223 (w), 1185(s), 1076 (m), 1040 (s), 1028 (w), 923 (w), 905 (w), 870 (w), 843 (m), 813 (m), 785 (m), 765 (w), 755 (w), 687 (m), 632 (m), 584 (w), 548 (w), 503 (w), 470 (w), 452 (w), 428 (w), 424 (w); **JXNU-7**(Sm), 3423 (s), 1599 (m), 1533 (s), 1442 (m), 1418 (w), 1392 (s), 1341 (m), 1184 (s), 1148 (w), 1081 (m), 1050 (s), 1029 (m), 926 (w), 906 (w), 838 (m), 814 (m), 768 (m), 681 (m), 632 (m), 591 (w), 547 (w), 524 (w), 498 (w), 451 (m); **JXNU-7**(Eu), 3453 (s), 1638 (m), 1532 (s), 1448 (w), 1423 (s), 1396 (m), 1377 (w), 1337 (m), 1200 (s), 1182 (s), 1075 (m), 1050 (s), 1028 (w), 876 (w), 843 (m), 810 (w), 772 (m), 683 (w), 638 (m), 589 (w), 541 (w), 523 (w), 499 (w), 445 (w).

Synthesis of $\{[Ln_4(\mu_3\text{-}OH)_4(DSNPDC)_2(H_2O)_{11}]\cdot 28H_2O\}_n$ (JXNU-8; Ln = Eu^{3+}, Gd^{3+}). A mixture of $Ln(NO_3)_3\cdot 6H_2O$ (0.01 mmol) and 5,7-disulfonate-1,4-naphthalenedicarboxylic acid (3.76 mg, 0.01 mmol) in 6 mL of H_2O/CH_3CN mixed solvent (v/v = 1/1) was introduced into a 20 mL Parr Teflon-lined stainless steel vessel, which was capped tightly and warmed to 100 °C for 3 days. Colorless crystals were obtained and dried in air. Yield based on the $Ln(NO_3)_3\cdot 6H_2O$: 55% for **JXNU-8**(Eu) and 36% for **JXNU-8**(Gd). Anal. Calcd/found for $C_{24}H_{90}O_{63}S_4Eu_4$ (2123.04): H, 4.27/4.16; C, 13.57/13.66; S, 6.04/5.98; Eu, 28.63/28.72. Calcd/found for $C_{24}H_{90}O_{63}S_4Gd_4$ (2144.19): H, 4.23/4.16; C, 13.44/13.28; S, 5.98/5.91; Gd, 29.33/29.19. IR (cm^{-1}, KBr pellet): **JXNU-8**(Eu), 3742 (w), 3437 (s), 1637 (w), 1567 (s), 1499 (w), 1446 (m), 1401 (s), 1341 (s), 1226 (w), 1181 (m), 1077 (m), 1043 (s), 1027 (w), 878 (w), 836 (w), 775 (w), 746 (w), 683 (m), 628 (m), 593 (w), 537 (w), 510 (w), 493 (w), 451 (w), 422 (w); **JXNU-8**(Gd), 3450 (s), 2977 (w), 1573 (s), 1498 (w), 1446 (m), 1401 (s), 1342 (m), 1227 (w), 1182 (m), 1076 (m), 1043 (s), 879 (w), 779 (w), 746 (w), 684 (w), 627 (m), 592 (w), 549 (w), 447 (w).

X-ray Crystallography. Single-crystal X-ray diffraction experiments were carried out on a Rigaku Oxford SuperNova diffractometer or a XtaLAB diffractometer (Mo Kα radiation, $\lambda = 0.71073$ Å). The structures were solved with SHELXT[15] and refined by the full-matrix least-squares method on F^2 using SHELXTL.[16] For **JXNU-7**, non-hydrogen atoms were refined anisotropically except for some carbon and oxygen atoms, which were refined isotopically to avoid "non-positive definite" results. For **JXNU-8**, all atoms except for hydrogen atoms were refined anisotropically. The hydrogen atoms attached to carbon atoms were assigned to calculated positions. Hydroxyl H and water H atoms were not located but are included in the formulas. The guest water molecules for **JXNU-8** are highly disordered and could not be modeled. Thus, the refinements of the structures of **JXNU-8** were further performed by ignoring the contribution of the disordered guest water molecules with PLATON.[17] The crystal data are summarized in Tables 1 and 2, and the important bond lengths are provided in Table S1.

RESULTS AND DISCUSSION

Crystal Structure Descriptions. The four compounds of **JXNU-7** revealed by X-ray single-crystal diffraction analyses are isostructural (Table 1). The slight difference between the

https://dx.doi.org/10.1021/acs.inorgchem.0c00680
Inorg. Chem. XXXX, XXX, XXX−XXX

Table 1. Crystallographic Data for JXNU-7[a]

	JXNU-7(La)	JXNU-7(Nd)	JXNU-7(Sm)	JXNU-7(Eu)
formula	$C_{24}H_{37}O_{35}S_4La_3$	$C_{24}H_{31}O_{32}S_4Nd_3$	$C_{24}H_{31}O_{32}S_4Sm_3$	$C_{24}H_{31}O_{32}S_4Eu_3$
fw	1430.50	1392.45	1410.78	1415.61
temp (K)	293(2)	293(2)	293(2)	293(2)
cryst syst	monoclinic	monoclinic	monoclinic	monoclinic
space group	$P2_1$	$P2_1$	$P2_1$	$P2_1$
Z	2	2	2	2
a (Å)	7.1983(3)	7.1126(5)	7.07610(10)	7.0508(4)
b (Å)	24.1419(10)	24.0391(16)	23.9242(5)	23.8840(9)
c (Å)	11.8444(6)	11.7687(8)	11.7549(2)	11.7398(4)
α (deg)	90	90	90	90
β (deg)	92.530(4)	92.582(6)	92.739(2)	92.732(4)
γ (deg)	90	90	90	90
V (Å^3)	2056.32(16)	2010.2(2)	1987.71(6)	1974.75(15)
D_{calcd} (g cm^{-3})	2.310	2.301	2.357	2.381
μ (mm^{-1})	3.381	4.135	4.695	5.030
no. of rflns collected	11857	14251	22986	13600
no. of indep rflns	7386	7605	7851	7299
no. of obsd rflns ($I > 2\sigma(I)$)	7152	6922	7626	6661
$F(000)$	1392	1350	1362	1368
R_{int}	0.0326	0.0667	0.0393	0.0470
R1 ($I > 2\sigma(I)$)[a]	0.0458	0.0804	0.0279	0.0447
wR2 (all data)[a]	0.1159	0.1898	0.0715	0.1048
CCDC no.	1987323	1987324	1987325	1987326

[a]R1 = $\sum||F_o| - |F_c||/\sum|F_o|$ and wR2 = $\{\sum[w(F_o^2 - F_c^2)^2]/\sum[w(F_o^2)^2]\}^{1/2}$.

Table 2. Crystallographic Data for JXNU-8

	JXNU-8(Eu)	JXNU-8(Gd)
formula	$C_{24}H_{34}O_{35}S_4Eu_4$	$C_{24}H_{34}O_{35}S_4Gd_4$
fw	1618.59	1639.75
temp (K)	293(2)	293(2)
cryst syst	orthorhombic	orthorhombic
space group	*Pnma*	*Pnma*
Z	4	4
a (Å)	19.8349(7)	19.7687(6)
b (Å)	20.9065(6)	20.8382(6)
c (Å)	18.0558(7)	17.9667(5)
α (deg)	90	90
β (deg)	90	90
γ (deg)	90	90
V (Å^3)	7487.3(4)	7401.3(4)
D_{calcd} (g cm^{-3})	1.436	1.472
μ (mm^{-1})	3.481	3.716
no. of rflns collected	40619	32345
no. of indep rflns	7861	7777
no. of obsd rflns ($I > 2\sigma(I)$)	6287	5838
$F(000)$	3096	3112
R_{int}	0.0753	0.0568
R1 ($I > 2\sigma(I)$)	0.0483	0.0416
wR2 (all data)	0.1198	0.0987
CCDC no.	1987327	1987328

lanthanum analogue and the other three compounds is that the lanthanum compound has one additional coordinated water molecule at the La1 center (Figure S1 in the Supporting Information) and two more lattice water molecules. Thus, **JXNU-7**(La) has a different thermal behavior in comparison with its analogues (Figure S2). **JXNU-7** has a 3D structure featuring linear trinuclear Ln_3 clusters acting as secondary building units (SBUs). The asymmetric unit of **JXNU-7**

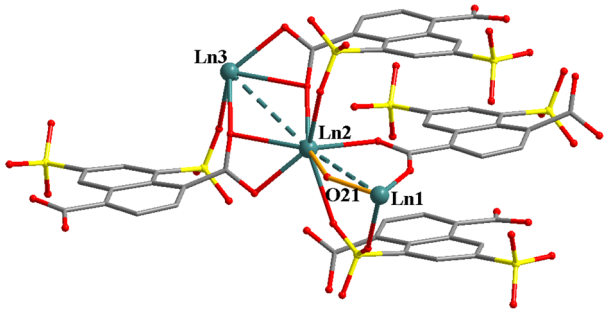

Figure 1. Linear trinuclear Ln_3 unit in **JXNU-7**.

consists of three Ln^{3+} ions, one μ_2-OH, two $DSNPDC^{4-}$ ligands, nine water ligands, and two lattice water molecules. The three crystallographically unique Ln^{3+} atoms are bridged by a hydroxyl group and the carboxylate and sulfonate groups to form a linear trinuclear Ln_3 unit, as displayed in Figure 1. The Ln1 atom is bonded to eight oxygen atoms from four water molecules, one μ_2-OH group, two sulfonate groups of two $DSNPDC^{4-}$ ligands, and one carboxylate group of the third $DSNPDC^{4-}$ ligand (Figure S1). The Ln2 and Ln3 atoms are nine-coordinated. Two water oxygen atoms, one hydroxyl oxygen atom, four carboxylate oxygen atoms, and two sulfonate oxygen atoms of four $DSNPDC^{4-}$ ligands occupy the coordination sites of the Ln2 atom (Figure S1). For the Ln3 atom, the nine-coordinated atoms are three water oxygen atoms, four carboxylate oxygen atoms, and two sulfonate oxygen atoms of four $DSNPDC^{4-}$ ligands. Two types of $DSNPDC^{4-}$ ligands exhibit different coordination modes. One has a μ_2-η^2:η^1 and unidentate mode of carboxylate groups and a μ_3-η^1:η^1:η^1 sulfonate group bridges five Ln^{3+} atoms with the second sulfonate group being uncoordinated (Figure S3a). The other contains μ_2-η^2:η^1 and μ_2-η^1:η^1 modes of carboxylate groups, one μ_2-η^1:η^1 sulfonate group, and one unidentate

https://dx.doi.org/10.1021/acs.inorgchem.0c00680
Inorg. Chem. XXXX, XXX, XXX−XXX

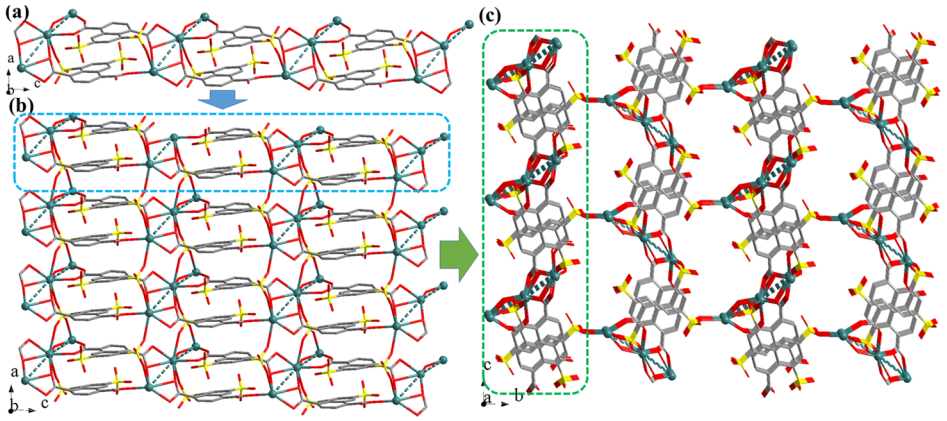

Figure 2. (a) 1D ribbon, (b) 2D layer, and (c) 3D structure of **JXNU-7**. H atoms and water molecules are omitted for clarity.

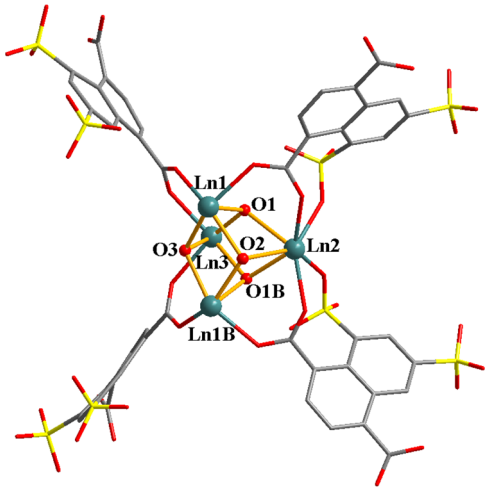

Figure 3. Cubic tetranuclear $Ln_4(\mu_3\text{-}OH)_4$ unit in **JXNU-8**.

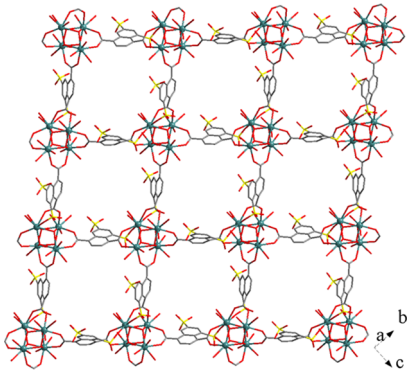

Figure 4. 2D square-grid layer of **JXNU-8**. H atoms are omitted for clarity.

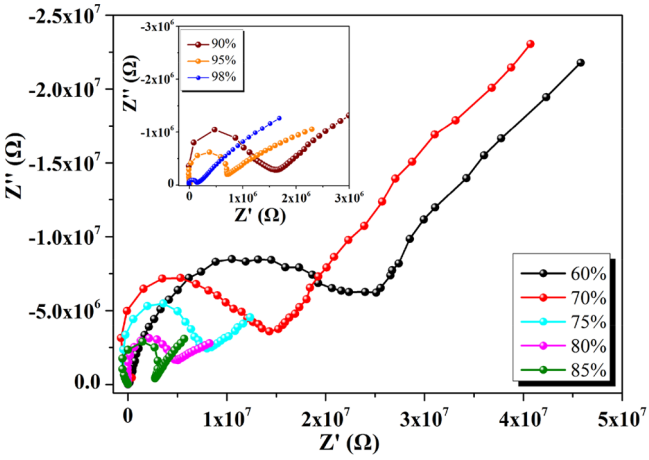

Figure 5. Nyquist plots of **JXNU-7**(Eu) at 85 °C at various RHs.

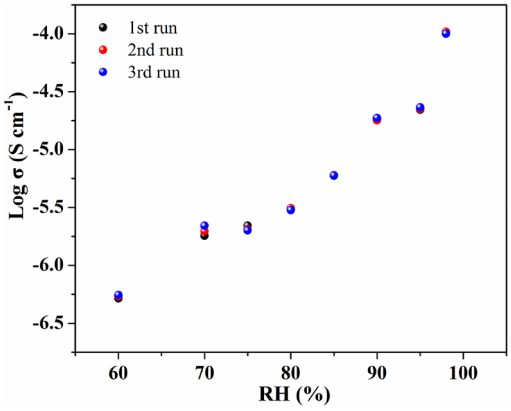

Figure 6. log σ versus RH plot of **JXNU-7**(Eu) at 85 °C with three cycles.

sulfonate group, bridging six lanthanide ions (Figure S3b). The Ln1, Ln2, and Ln3 atoms are connected by the carboxylate and sulfonate groups and a hydroxyl group to generate a linear trinuclear Ln_3 SBU. The linear trinuclear Ln_3 SBUs are interconnected by the carboxylate groups of the $DSNPDC^{4-}$ ligands to give a 1D ribbon extending along the *c* axis (Figure 2a). The adjacent 1D ribbons are held together through the bridging sulfonate groups with $\mu_3\text{-}\eta^1\text{:}\eta^1\text{:}\eta^1$ and $\mu_2\text{-}\eta^1\text{:}\eta^1$ coordination modes to form a 2D layer running along the *ac* plane (Figure 2b). As described above, the $DSNPDC^{4-}$ ligands using the carboxylate groups and $\mu_3\text{-}\eta^1\text{:}\eta^1\text{:}\eta^1$ and $\mu_2\text{-}\eta^1\text{:}\eta^1$ sulfonate groups link the Ln_3 units to give the 2D layer. The 2D layers are further interconnected through Ln−O bonds between Ln^{3+} atoms and the unidentate sulfonate groups of the neighboring 2D layers, forming the final 3D structure (Figure 2c and Figure S4). As is well-known, it is difficult to deliberately design the resulting structures of the lanthanide compounds due to the hard-sphere behavior of the lanthanide ions, which leads to difficulty in controlling the directionality of the coordinated ligands. The 1D lanthanide carboxylate

https://dx.doi.org/10.1021/acs.inorgchem.0c00680
Inorg. Chem. XXXX, XXX, XXX−XXX

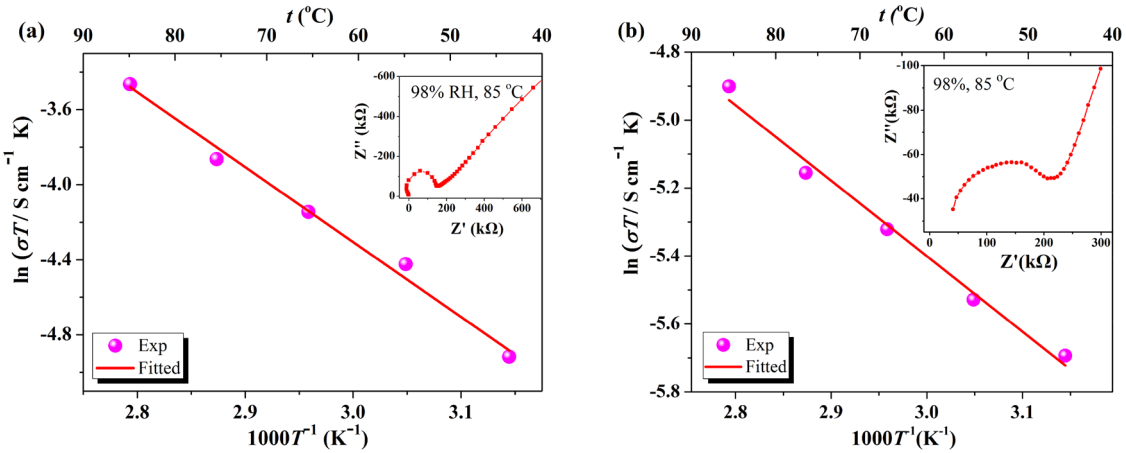

Figure 7. Arrhenius plots for **JXNU-7**(Eu) (a) and **JXNU-8**(Eu) (b) at an RH value of 98%. Each data point is the average value of three independent measurements. Insets: Nyquist plots for **JXNU-7**(Eu) and **JXNU-8**(Eu).

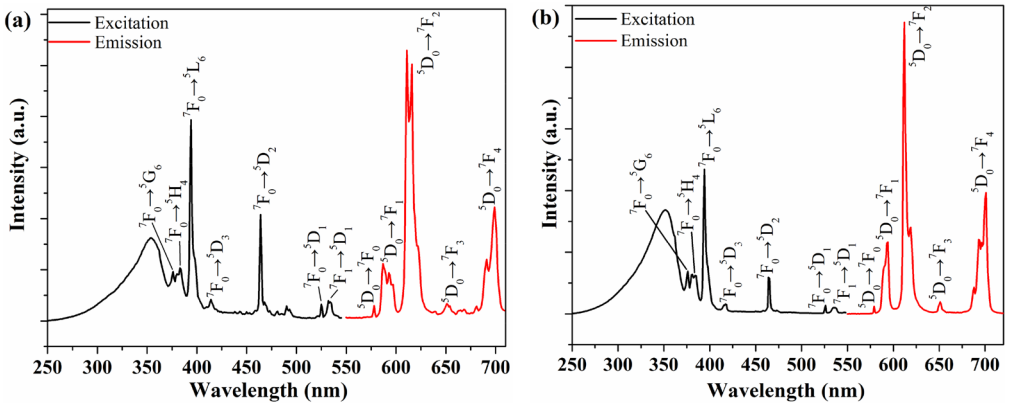

Figure 8. Excitation and emission spectra of **JXNU-7**(Eu) (a) and **JXNU-8**(Eu) (b).

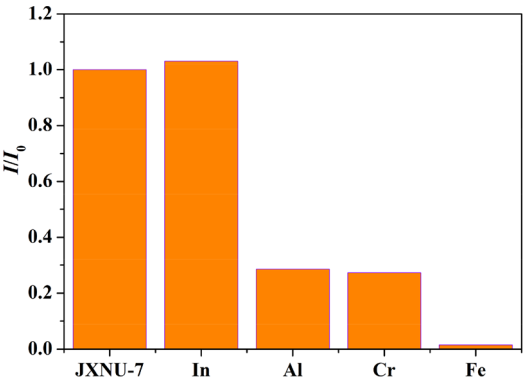

Figure 9. Integrated intensities of the $^5D_0 \rightarrow {}^7F_2$ (600−630 nm) emission band for **JXNU-7**(Eu) in the presence of trivalent metal ions (1 mM). I_0 and I represent the integrated intensities of **JXNU-7**(Eu) and **JXNU-7**(Eu) in the presence of the trivalent metal ions.

chains are the commonly observed SBUs for the lanthanide carboxylate frameworks. In addition, recently, there have been a few highly connected cluster-based MOFs reported with hexanuclear and nonanuclear lanthanide carboxylate clusters.[9b,10c] For the present case, the basic unit of the 3D framework is the linear trinuclear Ln_3 unit, which is a rare example of a 3D lanthanide carboxylate framework, enriching the scope of lanthanide carboxylate frameworks.

The two isostructural compounds of **JXNU-8** (Table 2) feature a 2D square-grid layer built from cubic tetranuclear $Ln_4(\mu_3\text{-OH})_4$ clusters. Three Ln^{3+} atoms, three μ_3-OH groups, one $DSNPDC^{4-}$ ligand, and eleven coordinated water molecules are in the asymmetric unit. The Ln2 and Ln3 atoms, O2 and O3 atoms of the μ_3-OH groups, and the coordinated water oxygen atoms O4W, O5W, and O7W are located in a mirror plane (Figure 3 and Figure S5). As a result, these atoms have a half-occupation in the asymmetric unit. Ln1 and Ln3 atoms, exhibiting similar coordination environments, are eight-coordinated, and each binds three hydroxyl oxygen atoms (O1, O2, and O3), three water oxygen atoms, and two carboxylate oxygen atoms of two $DSNPDC^{4-}$ ligands (Figure S5). The Ln2 atom is surrounded by nine coordinating atoms comprised of three hydroxyl oxygen atoms, two water oxygen atoms, two sulfonate oxygen atoms, and two carboxylate oxygen atoms of two $DSNPDC^{4-}$ ligands. As illustrated in Figure 3, four tridentate hydroxyl oxygen atoms bridge four Ln^{3+} atoms to give a cubic $Ln_4(\mu_3\text{-OH})_4$ cluster. The $Ln_4(\mu_3\text{-OH})_4$ unit has a symmetry of a crystallographically imposed mirror plane passing through Ln2, Ln3, O2, and O3 atoms (Figure 3). Four of the six edges of the Ln_4 tetrahedron embedded in a $Ln_4(\mu_3\text{-OH})_4$ cluster are bridged by four carboxylate arms. The $DSNPDC^{4-}$ ligand in **JXNU-8** binds four lanthanide ions with two μ_2-η^1:η^1 carboxylate groups and one unidentate sulfonate group. The remaining sulfonate group is not involved in coordination (Figure S3c). Each $Ln_4(\mu_3\text{-OH})_4$ cluster is bridged by four $DSNPDC^{4-}$ ligands to

https://dx.doi.org/10.1021/acs.inorgchem.0c00680
Inorg. Chem. XXXX, XXX, XXX−XXX

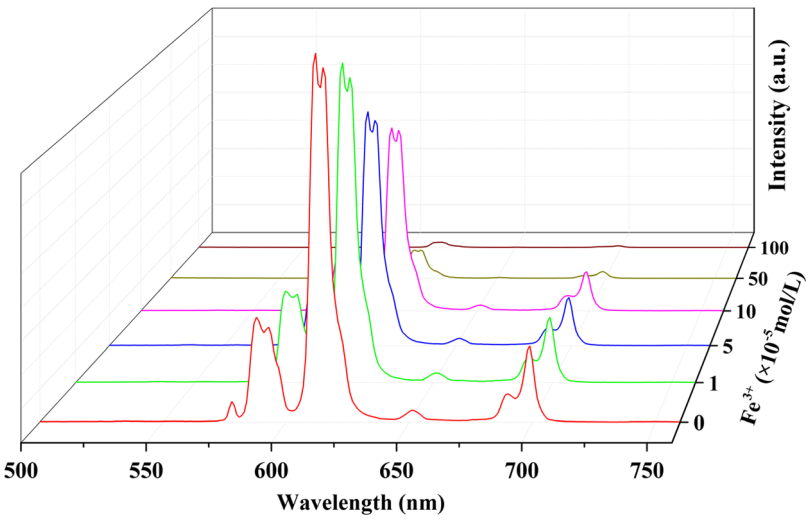

Figure 10. Emission spectra of **JXNU-7**(Eu) in the presence of Fe^{3+}.

generate a 2D square grid (Figure 4). The nanosized cavities of the 2D square-grid layer are filled by the disordered guest water molecules. Careful exploration of the 2D layer revealed that the free sulfonate groups point to the surfaces of the 2D layer (Figure S6). Thus, the interlayered spaces are full of sulfonate oxygen atoms (Figure S7).

Proton Conductivity. As described above, the two series of compounds are constructed from the sulfonate-carboxylate ligand with free sulfonate oxygen atoms and plenty of water molecules, implying that the present compounds are potential candidates for good proton conductors. The proton conduction of **JXNU-7**(Eu) with a good yield thus was explored as a representative. The proton-conducting behavior of **JXNU-7**(Eu) was studied with alternating current impedance spectroscopy on pellet samples. First, the equilibrium time of the humidity and temperature for the pellet sample was evaluated. As depicted in Figure S8, the proton conductivities of **JXNU-7**(Eu) are almost constant when the pellet sample was kept in the incubator for 4−25 h. Such a phenomenon indicates that the saturation of the sample needs at least 4 h. Thus, each alternating current impedance data of **JXNU-7**(Eu) was collected at an interval time of 5 h. The Nyquist plots obtained at 85 °C and varying relative humidities (RHs) were studied. The Nyquist plots show irregular electrochemical data when the RH is lower than 60%. When the RH is greater than 60%, the impedance plots exhibit an arch in the high-frequency region and a spike in the low-frequency range (Figure 5), which is a characteristic curve for a proton conductor. Upon an increase in the humidity, a decrease in the radius of the arcs is observed, which indicates that the proton conductivity (σ) is increased with an increase in humidity. The σ value at 98% RH (1.04×10^{-4} S cm^{-1}) is much higher than that at 60% RH (5.19×10^{-7} S cm^{-1}), suggesting that the proton conductivity of **JXNU-7**(Eu) is highly humidity dependent. The σ value of **JXNU-7**(Eu) at 98% RH and 85 °C is close to those of a Tb carboxylate sulfonate compound (6.57×10^{-4} S cm^{-1})[18] and a Gd oxalate compound (4.7×10^{-4} S cm^{-1})[19] under similar conditions. It has been reported that the classic MOFs MIL-53[20] and HKUST-1[21] have low σ values of 3.6×10^{-7} and 5×10^{-7} S cm^{-1}, respectively. However, it has been documented that the proton conductivities can be enhanced by encapsulation of H_2SO_4, a dye with a sulfonate group, or imidazole into the pores of the MOFs.[22]

In addition, the impedance data of **JXNU-7**(Eu) under 85 °C between RHs of 60% and 98% were collected repeatedly. The σ values at each RH show almost negligible changes in the repeated measurements (Figure 6). Such a behavior implies that the proton conductivity of **JXNU-7**(Eu) material has a good reproducibility, which is essential for a proton-conducting material. The PXRD pattern of the sample after impedance measurement is similar to the pattern of the pristine sample (Figure S9), implying the structural integrity of the **JXNU-7**(Eu) was retained in the impedance measurements.

Finally, the impedance data of **JXNU-7**(Eu) were recorded at 98% RH between 45 and 85 °C (Figure S10). Upon an increase in the temperature, the observation of a decrease in the size of the arc in the Nyquist plots indicates an increase in the proton conductivity. The enhancement of the proton conductivity with an increase in temperature can be ascribed to the thermal activation of water molecules. The activation energy E_a for proton transfer can be fitted from the temperature-dependent conductivity data using eq 1. By linear fitting of $\ln(\sigma T)$ versus $1000T^{-1}$ (Figure 7a), the E_a value for **JXNU-7**(Eu) was estimated to be 0.34 eV. The E_a value is less than 0.4 eV, which means that a Grotthuss mechanism[18] dominates the proton transfer in **JXNU-7**(Eu). As seen in the 3D structure of **JXNU-7**(Eu), the guest water molecules fill the 1D small channels and the coordinated water molecules and free sulfonate oxygen atoms point to the channel, giving a highly hydrophilic environment for the 1D channels. Careful exploration of the 1D small channels shows extensive hydrogen bonds between water molecules, including solvent water and coordinated water molecules, and sulfonate oxygen and carboxylate oxygen atoms and between water molecules (Table S2). These hydrogen bonds link the water oxygen atoms and sulfonate oxygen atoms as well as carboxylate oxygen atoms to generate a 1D hydrogen-bonded network in the 1D small channel (Figure S4b). The continuous hydrogen-bonded networks in the channels facilitate a fast and efficient proton transfer, resulting in a Grotthuss mechanism for **JXNU-7**(Eu).

$$\sigma = \frac{\sigma_0}{T} \exp\left(\frac{-E_a}{kT}\right) \quad (1)$$

https://dx.doi.org/10.1021/acs.inorgchem.0c00680
Inorg. Chem. XXXX, XXX, XXX−XXX

For the 2D layered structures of **JXNU-8**, **JXNU-8**(Eu) was selected for impedance measurements. The equilibrium time of temperature and humidity for the pellet sample of **JXNU-8**(Eu) is 2 h (Figure S11). **JXNU-8**(Eu) also displays the characteristic Nyquist plots of proton-conductive materials (Figure S12). At 85 °C, its proton conductivity increases from 1.86×10^{-7} S cm^{-1} at 65% RH to 2.23×10^{-5} S cm^{-1} at 98% RH, indicating a humidity-dependent proton conductivity. Under 98% RH, the σ value of **JXNU-8**(Eu) is enhanced from 45 °C (1.06×10^{-5} S cm^{-1}) to 85 °C (2.28×10^{-5} S cm^{-1}) (Figure S13). The proton conductivity of **JXNU-8**(Eu) also shows a good reproducibility at different RHs (Figure S14). The E_a value of **JXNU-8**(Eu) can be estimated from the temperature-dependent productivity at 98% RH (Figure 7), which gives an E_a value of 0.18 eV. Similar to that of **JXNU-7**(Eu), **JXNU-8**(Eu) displays a Grotthuss-type proton transport mechanism. As shown in Figure S6, the free sulfonate groups and free sulfonate oxygen atoms as well as the coordinated water molecules point to either side of the 2D layers, thus giving highly hydrophilic interlayered spaces (Figure S7). The solvent water molecules located at the interlayered spaces form hydrogen bonds with sulfonate oxygen and coordinated water molecules to provide proton transfer pathways. These proton conductivities of **JXNU-8**(Eu) are smaller than those of **JXNU-7**(Eu) at the same temperature and humidity, which is the result of the different structures. The 1D channels including the 1D ordered hydrogen-bonded networks in **JXNU-7**(Eu) facilitate fast proton transport, resulting in a high proton conductivity for **JXNU-7**(Eu).

Photoluminescent Properties. Eu^{3+}-based MOFs can emit a characteristic red color, which enables them to be potentially used as luminescence probes and display devices. The photoluminescent properties of compounds **JXNU-7**(Eu) and **JXNU-8**(Eu) were explored. First, the excitation and emission spectra of the H_4-DSNPDC organic ligand were examined in the solid state. Upon excitation at 367 nm, the organic ligand emits a photoluminescent emission band with a maximum intensity at 418 nm, which is ascribed to an intraligand $\pi^*-\pi$ electron transition (Figure S15). Figure 8 shows the solid-state excitation and emission spectra for **JXNU-7**(Eu) and **JXNU-8**(Eu) at room temperature. An excitation band from 300 to 370 nm accompanied by sharp peaks was observed for **JXNU-7**(Eu) (Figure 8a). The excitation band ranging from 300 to 370 nm can be attributed to a ligand-centered transition. The sharp lines are the intra-4f^6 transitions of an Eu^{3+} ion between the $^7F_{0,1}$ level and the $^5H_4$, $^5L_6$, and ^5D_J (J = 3, 2, 1) levels (Figure 8a).[23] **JXNU-7**(Eu) shows the characteristic Eu^{3+} emission on excitation at 355 nm. It is known that the $^5D_0$ emitting level for Eu^{3+} is at 17267 cm^{-1}.[24] The observed intense Eu^{3+} emission for **JXNU-7**(Eu) suggests that the triplet excited state T_1 level for the organic ligand is higher than that of the Eu^{3+} emitting level. As shown in Figure 8a, the emission spectrum is dominated by the peak of a $^5D_0 \rightarrow {}^7F_2$ electric-dipole transition, which is sensitive to the site symmetry of the Eu^{3+} ion. For **JXNU-7**(Eu), the integrated intensity ratio between the $^5D_0 \rightarrow {}^7F_2$ transition and the magnetic dipole $^5D_0 \rightarrow {}^7F_1$ transition is 4.8, which suggests a low-symmetry site for the Eu^{3+} ions in **JXNU-7**(Eu). In addition, the presence of the $^5D_0 \rightarrow {}^7F_0$ transition indicates that the Eu^{3+} ions are located in a C_s, C_n, or C_{nv} symmetry site. As mentioned above, **JXNU-7**(Eu) crystallizes in the monoclinic $P2_1$ space group with three crystallographically unique Eu^{3+} atoms lying on general positions, indicating that the site symmetry for Eu^{3+} ions belongs to C_1. Finally, the observation of the splitting of $^5D_0 \rightarrow {}^7F_1$, $^5D_0 \rightarrow {}^7F_2$, and $^5D_0 \rightarrow {}^7F_4$ peaks further corroborates the low site symmetry for the Eu^{3+} ions.[25]

The profiles of the excitation and emission spectra for **JXNU-8**(Eu) are similar to those of **JXNU-7**(Eu). On excitation at 352 nm, **JXNU-8**(Eu) exhibits intense Eu^{3+} luminescence with an integrated intensity ratio between the $^5D_0 \rightarrow {}^7F_2$ and $^5D_0 \rightarrow {}^7F_1$ transitions of 3.6 (Figure 8b).

As described above, **JXNU-7**(Eu) is a 3D structure with small 1D channels (Figure 2c), while **JXNU-8**(Eu) is a 2D layer with close-packed layers. Such small channels of **JXNU-7**(Eu) are suitable for accommodating the guest metal ions, indicating that **JXNU-7**(Eu) is a promising candidate for serving as a luminescence probe for metal ions. The luminescent sensing of the trivalent metal ions In^{3+}, Al^{3+}, Cr^{3+}, and Fe^{3+} for **JXNU-7**(Eu) was studied. As depicted in Figure S16, the characteristic Eu^{3+} luminescence can be observed on addition of the trivalent metal ions (metal ion concentration 1 mM) to an aqueous suspension of **JXNU-7**(Eu) (concentration 1 mg/mL). The Eu^{3+} luminescence is not affected by In^{3+} (Figure 9), while the other three metal ions quench the luminescence of **JXNU-7**(Eu) to different extents. The addition of Fe^{3+} weakens the luminescence intensity of **JXNU-7**(Eu) completely (Figure 9). Thus, the luminescence quenching for **JXNU-7**(Eu) in the presence of Fe^{3+} was studied further. As illustrated in Figure 10, the emission intensity of **JXNU-7**(Eu) is gradually weakened with an increase in the concentration of Fe^{3+}. Furthermore, anti-interference experiments were carried out. The results showed that the quenching of the emission intensity of **JXNU-7**(Eu) induced by Fe^{3+} is not affected in the presence of other trivalent metal ions (Figure S17). The PXRD pattern of **JXNU-7**(Eu) with Fe^{3+} matches well with that of the pristine **JXNU-7**(Eu) (Figure S9). Such a result indicates that the 3D structure of **JXNU-7**(Eu) was retained after the addition of Fe^{3+} and a luminescence quenching effect of Fe^{3+} resulting from the collapse of the 3D framework can be excluded. The lanthanide luminescence is generally derived from the energy transfer from organic ligands to the Ln^{3+} ions. As depicted in Figure S18, the UV−vis absorption spectra of the metal ions in aqueous solutions showed that the absorption band of **JXNU-7**(Eu) (265−360 nm) is overlapped with the absorption band of Fe^{3+} ion (250−400 nm). Such a result implies that the Fe^{3+} aqueous solution could absorb the energy of the excitation light of **JXNU-7**(Eu), leading to a reduction of the energy transfer from organic ligands to the Eu^{3+} centers. As a result, the Eu^{3+} luminescence is quenched. Thus, **JXNU-7**(Eu) acting as a probe is preferred for Fe^{3+} detection.

CONCLUSIONS

In conclusion, a sulfonate-carboxylate ligand and its lanthanide-based frameworks **JXNU-7** and **-8** have been synthesized. **JXNU-7** has a 3D structure constructed from linear trinuclear lanthanide carboxylate units, while **JXNU-8** has a 2D layered structure based on tetranuclear $Ln_4(\mu_3\text{-OH})_4$ cluster units. The Eu analogues exhibit good proton-conducting performance pertaining to the hydrophilic sulfonate groups. **JXNU-7**(Eu) with its characteristic emission serves as a luminescent sensor for the selective recognition of Fe^{3+} ion in aqueous solution. Our work is an elegant demonstration of the realization of the functionalities endowed by the functional building units in the resulting MOFs.

https://dx.doi.org/10.1021/acs.inorgchem.0c00680
Inorg. Chem. XXXX, XXX, XXX−XXX

■ ASSOCIATED CONTENT

Supporting Information

The Supporting Information is available free of charge at https://pubs.acs.org/doi/10.1021/acs.inorgchem.0c00680.

Bond lengths, proton conduction, TGA curves, luminescence spectra, PXRD patterns, UV−vis adsorption spectra, and IR spectra (PDF)

Accession Codes

CCDC 1987323−1987328 contain the supplementary crystallographic data for this paper. These data can be obtained free of charge via www.ccdc.cam.ac.uk/data_request/cif, or by emailing data_request@ccdc.cam.ac.uk, or by contacting The Cambridge Crystallographic Data Centre, 12 Union Road, Cambridge CB2 1EZ, UK; fax: +44 1223 336033.

■ AUTHOR INFORMATION

Corresponding Authors

Yu-Ling Wang − *College of Chemistry and Chemical Engineering, Jiangxi Normal University, Nanchang 330022, Jiangxi, People's Republic of China;* orcid.org/0000-0002-0839-699X; Email: ylwang@jxnu.edu.cn

Qing-Yan Liu − *College of Chemistry and Chemical Engineering, Jiangxi Normal University, Nanchang 330022, Jiangxi, People's Republic of China;* orcid.org/0000-0003-1991-792X; Email: qyliuchem@jxnu.edu.cn

Authors

Meng-Ye Xu − *College of Chemistry and Chemical Engineering, Jiangxi Normal University, Nanchang 330022, Jiangxi, People's Republic of China*

Qingyou Liu − *Institute of Geochemistry, Chinese Academy of Sciences, Guiyang 550081, Guizhou, People's Republic of China;* orcid.org/0000-0002-5630-7680

Zhao-Ting Lin − *College of Chemistry and Chemical Engineering, Jiangxi Normal University, Nanchang 330022, Jiangxi, People's Republic of China*

Complete contact information is available at: https://pubs.acs.org/10.1021/acs.inorgchem.0c00680

Notes

The authors declare no competing financial interest.

■ ACKNOWLEDGMENTS

This work was financially supported by the NNSF of China (Grants 21661014, 21861020, and 21561015) and the NSF of Jiangxi province (Grant 20171ACB20008 and 20181BAB203001).

■ REFERENCES

(1) (a) Li, H.; Wang, K.; Sun, Y.; Lollar, C. T.; Li, J.; Zhou, H. C. Recent advances in gas storage and separation using metal−organic frameworks. *Mater. Today* **2018**, *21*, 108−121. (b) He, Y. B.; Chen, F. L.; Li, B.; Qian, G. D.; Zhou, W.; Chen, B. L. Porous metal−organic frameworks for fuel storage. *Coord. Chem. Rev.* **2018**, *373*, 167−198.

(2) (a) Rocha, J.; Carlos, L. D.; Almeida Paz, F. A.; Ananias, D. Luminescent multifunctional lanthanides-based metal−organic frameworks. *Chem. Soc. Rev.* **2011**, *40*, 926−940. (b) Cui, Y.; Yue, Y.; Qian, G.; Chen, B. Luminescent Functional Metal−Organic Frameworks. *Chem. Rev.* **2012**, *112*, 1126−1162.

(3) (a) Liu, X.-J.; Zhang, Y.-H.; Chang, Z.; Li, A.-L.; Tian, D.; Yao, Z.-Q.; Jia, Y.-Y.; Bu, X.-H. A Water-Stable Metal−Organic Framework with a Double-Helical Structure for Fluorescent Sensing. *Inorg. Chem.* **2016**, *55*, 7326−7328. (b) Hao, J.-N.; Yan, B. Ag^{+}-sensitized in Ln^{3+} post-functionalized lanthanide luminescence metal−organic frameworks and Ag^{+} sensing. *J. Mater. Chem. A* **2015**, *3*, 4788−4792. (c) He, R.; Wang, Y.-L.; Ma, H.-F.; Yin, S.-G.; Liu, Q.-Y. Eu^{3+}-functionalized metal−organic framework composite as ratiometric fluorescent sensor for highly selective detecting urinary 1-hydroxypyrene. *Dyes Pigm.* **2018**, *151*, 342−347. (d) Chen, W.-M.; Meng, X.-L.; Zhuang, G.-L.; Wang, Z.; Kurmoo, M.; Zhao, Q.-Q.; Wang, X.-P.; Shan, B.; Tung, C.-H.; Sun, D. A superior fluorescent sensor for Al^{3+} and UO_2^{2+} based on a Co(II) metal−organic framework with exposed pyrimidyl Lewis base sites. *J. Mater. Chem. A* **2017**, *5*, 13079−13085.

(4) (a) Ramaswamy, P.; Wong, N. E.; Shimizu, G. K. H. MOFs as proton conductors−challenges and opportunities. *Chem. Soc. Rev.* **2014**, *43*, 5913−5932. (b) Meng, X.; Wang, H.-N.; Song, S.-Y.; Zhang, H.-J. Proton-conducting crystalline porous materials. *Chem. Soc. Rev.* **2017**, *46*, 464−480. (c) Xie, X.-X.; Yang, Y.-C.; Dou, B.-H.; Li, Z.-F.; Li, G. Proton conductive carboxylate-based metal−organic frameworks. *Coord. Chem. Rev.* **2020**, *403*, 213100. (d) Bao, S.-S.; Shimizu, G. K. H.; Zheng, L.-M. Proton conductive metal phosphonate frameworks. *Coord. Chem. Rev.* **2019**, *378*, 577−594. (e) Liu, D.-D.; Wang, Y.-L.; Luo, F.; Liu, Q.-Y. Rare Three-Dimensional Uranyl−Biphenyl-3,3′-disulfonyl-4,4′-dicarboxylate Frameworks: Crystal Structures, Proton Conductivity, and Luminescence. *Inorg. Chem.* **2020**, *59*, 2952−2960. (f) Ye, Y.; Guo, W.; Wan, L.; Li, Z.; Song, Z.; Chen, J.; Zhang, Z.; Xiang, S.; Chen, B. Straightforward Loading of Imidazole Molecules into Metal Organic Framework for High Proton Conduction. *J. Am. Chem. Soc.* **2017**, *139*, 15604−15607. (g) Liu, L.-Z.; Yao, Z.-Z.; Ye, Y.-X.; Lin, Q.-J.; Chen, S.-M.; Zhang, Z.-J.; Xiang, S.-C. Enhanced Intrinsic Proton Conductivity of Metal−Organic Frameworks by Tuning the Degree of Interpenetration. *Cryst. Growth Des.* **2018**, *18*, 3724−3728.

(5) (a) Sorace, L.; Benellib, C.; Gatteschi, D. Lanthanides in molecular magnetism: old tools in a new field. *Chem. Soc. Rev.* **2011**, *40*, 3092−3104. (b) Wang, Y.-L.; Han, C.-B.; Zhang, Y.-Q.; Liu, Q.-Y.; Liu, C.-M.; Yin, S.-G. Fine-Tuning Ligand to Modulate the Magnetic Anisotropy in a Carboxylate-Bridged Dy_2 Single-Molecule Magnets System. *Inorg. Chem.* **2016**, *55*, 5578−5584. (c) Li, R.-P.; Liu, Q.-Y.; Wang, Y.-L.; Liu, C.-M.; Liu, S.-J. Evolution from linear tetranuclear clusters into one-dimensional chains of Dy(III) single-molecule magnets with an enhanced energy barrier. *Inorg. Chem. Front.* **2017**, *4*, 1149−1156. (d) Wang, X.-P.; Chen, W.-M.; Qi, H.; Li, X.-Y.; Rajn, C.; Feng, Z.-Y.; Kurmoo, M.; Boča, R.; Jia, C.-J.; Tung, C.-H.; Sun, D. Solvent-Controlled Phase Transition of a Co^{II}-Organic Framework: From Achiral to Chiral and Two to Three Dimensions. *Chem. - Eur. J.* **2017**, *23*, 7990−7996.

(6) Horike, S.; Bureekaew, S.; Kitagawa, S. Coordination pillared-layer type compounds having pore surface functionalization by anionic sulfonate groups. *Chem. Commun.* **2008**, 471−473.

(7) Yang, F.; Huang, H.; Wang, X.; Li, F.; Gong, Y.; Zhong, C.; Li, J. R. Proton Conductivities in Functionalized UiO-66: Tuned Properties, Thermogravimetry Mass, and Molecular Simulation Analyses. *Cryst. Growth Des.* **2015**, *15*, 5827−5833.

(8) Bünzli, J.-C. G. Benefiting from the Unique Properties of Lanthanide Ions. *Acc. Chem. Res.* **2006**, *39*, 53−61.

(9) (a) Lustig, W. P.; Mukherjee, S.; Rudd, N. D.; Desai, A. V.; Li, J.; Ghosh, S. K. Metal−organic frameworks: functional luminescent and photonic materials for sensing applications. *Chem. Soc. Rev.* **2017**, *46*, 3242−3285. (b) Li, Y.-J.; Wang, Y.-L.; Liu, Q.-Y. The Highly Connected MOFs Constructed from Nonanuclear and Trinuclear Lanthanide-Carboxylate Clusters: Selective Gas Adsorption and Luminescent pH Sensing. *Inorg. Chem.* **2017**, *56*, 2159−2164. (c) Yang, Y.; Chen, L.; Jiang, F. L.; Yu, M. X.; Wan, X. Y.; Zhang, B.; Hong, M. C. A family of doped lanthanide metal−organic frameworks for wide-range temperature sensing and tunable white light emission. *J. Mater. Chem. C* **2017**, *5*, 1981−1989.

(10) (a) Zhang, Y.-B.; Furukawa, H.; Ko, N.; Nie, W.; Park, H. J.; Okajima, S.; Cordova, K. E.; Deng, H.; Kim, J.; Yaghi, O. M. Introduction of Functionality, Selection of Topology, and Enhancement of Gas Adsorption in Multivariate Metal−Organic Framework-

177. *J. Am. Chem. Soc.* **2015**, *137*, 2641−2650. (b) Deria, P.; Chung, Y. G.; Snurr, R. Q.; Hupp, J. T.; Farha, O. K. Water stabilization of Zr_6-based metal−organic frameworks via solvent-assisted ligand incorporation. *Chem. Sci.* **2015**, *6*, 5172−5176. (c) Xue, D.-X.; Cairns, A. J.; Belmabkhout, Y.; Wojtas, L.; Liu, Y.; Alkordi, M. H.; Eddaoudi, M. Tunable Rare-Earth fcu-MOFs: A Platform for Systematic Enhancement of CO_2 Adsorption Energetics and Uptake. *J. Am. Chem. Soc.* **2013**, *135*, 7660−7667.

(11) (a) Shimizu, G. K. H.; Vaidhyanathan, R.; Taylor, J. M. Phosphonate and sulfonate metal organic frameworks. *Chem. Soc. Rev.* **2009**, *38*, 1430−1449. (b) Sun, D.; Liu, F.-J.; Hao, H.-J.; Li, Y.-H.; Zhang, N.; Huang, R.-B.; Zheng, L.-S. A novel arenedisulfonate-templated 1D silver ladder constructed from 4-aminobenzonitrile ligand. *CrystEngComm* **2011**, *13*, 5661−5665. (c) Dong, X.-Y.; Wang, R.; Li, J.-B.; Zang, S.-Q.; Hou, H.-W.; Mak, T. C. W. A tetranuclear $Cu_4(\mu_3\text{-}OH)_2$-based metal−organic framework (MOF) with sulfonate−carboxylate ligands for proton conduction. *Chem. Commun.* **2013**, *49*, 10590−10592. (d) Wei, M.-J.; Fu, J.-Q.; Wang, Y.-D.; Zhang, Y.; Zang, H.-Y.; Shao, K.-Z.; Li, Y.-G.; Su, Z.-M. Highly tuneable proton-conducting coordination polymers derived from a sulfonate-based ligand. *CrystEngComm* **2017**, *19*, 7050−7056.

(12) (a) Yang, F.; Xu, G.; Dou, Y.; Wang, B.; Zhang, H.; Wu, H.; Zhou, W.; Li, J.-R.; Chen, B. A flexible metal−organic framework with a high density of sulfonic acid sites for proton conduction. *Nature. Energy.* **2017**, *2*, 877−883. (b) Zhou, L.-J.; Deng, W.-H.; Wang, Y.-L.; Xu, G.; Yin, S.-G.; Liu, Q.-Y. Lanthanide-Potassium-Biphenyl-3,3′-disulfonyl-4,4′-dicarboxylate Frameworks: Gas Sorption, Proton Conductivity, and Luminescent Sensing of Metal Ions. *Inorg. Chem.* **2016**, *55*, 6271−6277. (c) Wang, Z.-Q.; Zhou, L.-J.; Wang, Y.-L. A Dy(III)-K(I)-Biphenyl-3,3′-disulfonyl-4,4′-dicarboxylate Compound: Structure and Luminescence. *Chin. J. Struct. Chem.* **2019**, *38*, 1194−1199.

(13) (a) Maity, D. K.; Otake, K.; Ghosh, S.; Kitagawa, H.; Ghoshal, D. Sulfonic Group Functionalized Mixed Ligand Coordination Polymers: Synthesis, Characterization, Water Sorption, and Proton Conduction studies. *Inorg. Chem.* **2017**, *56*, 1581−1590. (b) Maity, D. K.; Ghosh, S.; Otake, K.; Kitagawa, H.; Ghoshal, D. Proton Conductivity and Sorption Study in Three Sulfonic Group Functionalized Mixed Ligand Coordination Polymers and the Impact of Structural Dynamicity on Their Property. *Inorg. Chem.* **2019**, *58*, 12943−12953.

(14) (a) Meng, X.; Song, S. Y.; Song, X. Z.; Zhu, M.; Zhao, S. N.; Wu, L. L.; Zhang, H. J. A tetranuclear copper cluster-based MOF with sulfonate−carboxylate ligands exhibiting high proton conduction properties. *Chem. Commun.* **2015**, *51*, 8150−8152. (b) Dong, X. Y.; Wang, R.; Wang, J. Z.; Zang, S. Q.; Mak, T. C. W. Highly selective Fe^{3+} sensing and proton conduction in a water-stable sulfonate−carboxylate Tb−organic-framework. *J. Mater. Chem. A* **2015**, *3*, 641−647.

(15) Sheldrick, G. M. SHELXT−Integrated space-group and crystal-structure determination. *Acta Crystallogr., Sect. A: Found. Adv.* **2015**, *A71*, 3−8.

(16) Sheldrick, G. M. Crystal structure refinement with SHELXL. *Acta Crystallogr., Sect. C: Struct. Chem.* **2015**, *71*, 3−8.

(17) Spek, A. L. *PLATON: A Multipurpose Crystallographic Tool*; Utrecht University: Utrecht, The Netherlands, 2001.

(18) Zhang, W.-W.; Wang, Y.-L.; Liu, Q.; Liu, Q.-Y. Lanthanide-benzophenone-3,3′-disulfonyl-4,4'-dicarboxylate Frameworks: Temperature and 1-Hydroxypyren Luminescence Sensing, and Proton Conduction. *Inorg. Chem.* **2018**, *57*, 7805−7814.

(19) Biswas, S.; Chakraborty, J.; Parmar, V. S.; Bera, S. P.; Ganguli, N.; Konar, S. Channel-Assisted Proton Conduction Behavior in Hydroxyl-Rich Lanthanide-Based Magnetic Metal−Organic Frameworks. *Inorg. Chem.* **2017**, *56*, 4956−4965.

(20) Shigematsu, A.; Yamada, T.; Kitagawa, H. Control of Proton Conductivity in Porous Coordination Polymers. *J. Am. Chem. Soc.* **2011**, *133*, 2034−2036.

(21) Jeong, N. C.; Samanta, B.; Lee, C. Y.; Farha, O. K.; Hupp, J. T. Coordination-Chemistry Control of Proton Conductivity in the Iconic Metal−Organic Framework Material HKUST-1. *J. Am. Chem. Soc.* **2012**, *134*, 51−54.

(22) (a) Li, X.-M.; Dong, L.-Z.; Li, S.-L.; Xu, G.; Liu, J.; Zhang, F.-M.; Lu, L.-S.; Lan, Y.-Q. Synergistic Conductivity Effect in a Proton Sources-Coupled Metal−Organic Framework. *ACS Energy Lett.* **2017**, *2*, 2313−2318. (b) Liu, L.-Z.; Yao, Z.-Z.; Ye, Y.-X.; Liu, C.-L.; Lin, Q.-J.; Chen, S.-M.; Xiang, S.-C.; Zhang, Z.-J. Enhancement of Intrinsic Proton Conductivity and Aniline Sensitivity by Introducing Dye Molecules into the MOF Channel. *ACS Appl. Mater. Interfaces* **2019**, *11*, 16490−16495. (c) Zhang, F.-M.; Dong, L.-Z.; Qin, J.-S.; Guan, W.; Liu, J.; Li, S.-L.; Lu, M.; Lan, Y.-Q.; Su, Z.-M.; Zhou, H.-C. Effect of Imidazole Arrangements on Proton-Conductivity in Metal−Organic Frameworks. *J. Am. Chem. Soc.* **2017**, *139*, 6183−6189.

(23) Albin, M.; Wright, R. R.; Horrocks, W. D. Laser Spectroscopic and X-ray Structural Investigation of Europium(III)-Oxydiacetate Complexes in Solution and in the Solid State. *Inorg. Chem.* **1985**, *24*, 4591−4594.

(24) Carnall, W. T.; Fields, P. R.; Rajnak, K. Electronic Energy Levels in the Trivalent Lanthanide Aquo Ions. I. Pr^{3+}, Nd^{3+}, Pm^{3+}, Sm^{3+}, Dy^{3+}, Ho^{3+}, Er^{3+}, and Tm^{3+}. *J. Chem. Phys.* **1968**, *49*, 4450−4455.

(25) (a) Marques, L. F.; Correa, C. C.; Ribeiro, S. J. L.; dos Santos, M. V.; Dutra, J. D. L.; Freire, R. O.; Machado, F. C. Synthesis, structural characterization, luminescent properties and theoretical study of three novel lanthanide metal-organic frameworks of Ho(III), Gd(III) and Eu(III) with 2,5-thiophenedicarboxylate anion. *J. Solid State Chem.* **2015**, *227*, 68−78. (b) Li, Z.-T.; Wang, Z.-Q.; Liu, Q.-Y.; Wang, Y.-L. Three-dimensional lanthanide frameworks constructed of two-dimensional squares strung on one-dimensional double chains: Syntheses, structures, and luminescent properties. *Inorg. Chim. Acta* **2019**, *484*, 13−18.

https://dx.doi.org/10.1021/acs.inorgchem.0c00680
Inorg. Chem. XXXX, XXX, XXX−XXX